SUPPLEMENTAL FIGURES

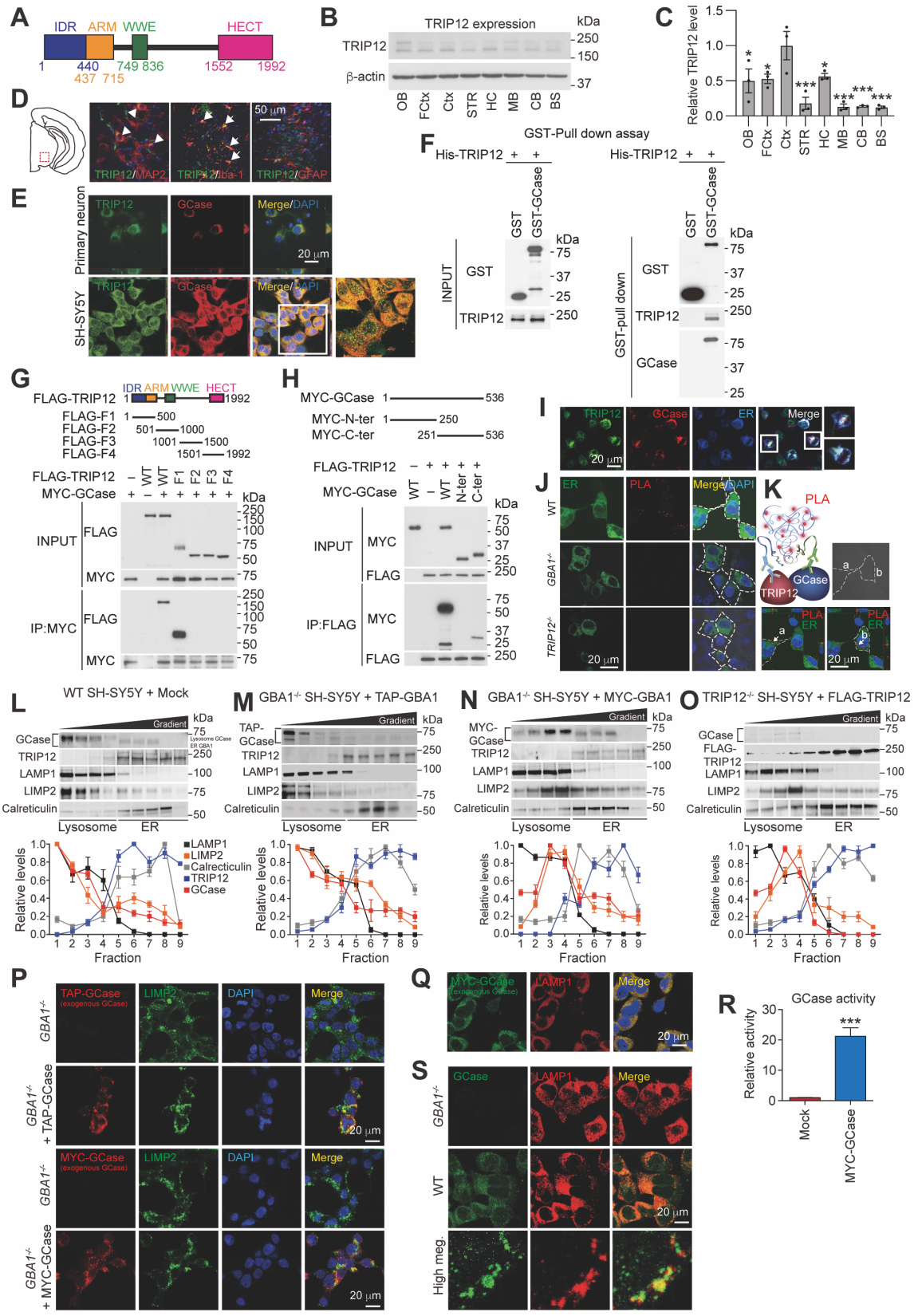

Figure S1. Identification of TRIP12 and binding domain between TRIP12 and GCase and validation for tagged constructs of TRIP12 and GCase (Related to Figure 1).

(A) Schematic diagram of the TRIP12 protein showing the IDR, ARM, WWE and HECT domain motifs.

(B) Regional analysis and levels of TRIP12 expression by western blot analysis.

(C) Levels of TRIP12 expression in each region were quantified as a bar graph (n=3, each group).

(D) Representative confocal images with anti-TRIP12 antibody along with various cell-type specific markers. The co-localization of TRIP12 (green) with neuronal (MAP2), microglial (Iba-1), or astroglial (GFAP) markers (red) was measured in the SNpc of wild-type mice.

(E) Representative confocal images with anti-TRIP12 and anti- GCase antibodies reveal that TRIP12 and GCase are co-localized mostly in primary cultured neurons or SH-SY5Y dopaminergic-like neurons.

(F) GST-pull-down assay between His-tagged TRIP12 and GST-tagged GCase, indicating an interaction between GCase and TRIP12.

(G) A full-length FLAG- tagging TRIP12 (FLAG-TRIP12) and N-terminal fragment of TRIP12 (FLAG-F1) interacts with GCase. Deletion mutants of FLAG-TRIP12 include the N-terminal fragment (F1), the intermediate domains (F2 and F3), or the C-terminal domain (F4) of TRIP12.

(H) A full-length MYC-tagging GCase (MYC-GCase) and C-terminal fragment of GCase (MYC-C-ter) interacts with TRIP12. Deletion mutants of MYC-GCase include N-terminal fragment of GCase (MYC-N-ter) or MYC-C-ter.

(I) Representative confocal image showing co-localization between TRIP12 and GCase in the ER. The SH-SY5Y cells were stained with anti-TRIP12, GCase, and Calreticulin antibodies for ER marker.

(J) The positive fluorescence signals in WT SH-SY5Y cells were eliminated in *GBA1* knockout (*GBA*$^{-/-}$) or *TRIP12* knockout (*TRIP12*$^{-/-}$) SH-SY5Y cells.

(K) Confocal z-stack images from the proximity ligation assay (PLA) shows that interaction between TRIP12 and GCase (a and b) occurs in the endoplasmic reticulum (ER) of WT SH-SY5Y cells.

(L) The intracellular localization of endogenous TRIP12 and GCase in SH-SY5Y with Mock through density gradient-based subcellular fractionation.

(M and N) Validation for tagged constructs of GCase. The intracellular localization of TAP-tagging (TAP-GCase) or MYC-tagging GCase (MYC-GCase) overexpressed *GBA1* knockout SH-SY5Y cells. TAP-GCase or MYC-GCase plasmids were transfected in *GBA1* knockout SH-SY5Y followed by iodixanol density gradient centrifugation.

(O) FLAG-TRIP12 plasmid was transfected in *TRIP12* knockout SH-SY5Y followed by gradient centrifugation (related to Supporting Figure 3).

(L-O) Isolated subcellular fractions (1 to 9) were subjected to western blot analysis using anti-GCase, TRIP12, MYC, FLAG, LAMP1, LIMP2, and Calreticulin antibodies. The proteins were quantified by the densitometric analysis of bands in digital images of western blots. For each given protein, the average density of each fraction was normalized to the high peak density of the protein and plotted as a line graph. (n=3, each fraction).

(P) The colocalization of TAP- or MYC-tagged GCase with LIMP2. TAP- or MYC-GCase were transfected in *GBA1* knockout SH-SY5Y cells for 48 hours. Representative confocal images with anti-GCase or MYC antibodies along with anti-LIMP2 antibody reveal that exogenous TAP- or MYC-GCase are co-localized with LIMP2 in *GBA1* knockout SH-SY5Y cells.
(Q) Representative confocal images with anti-MYC and anti-LAMP1 antibodies reveal that exogenous MYC-GCase are co-localized in the lysosomes of SH-SY5Y cells.
(R) Lysosomes were isolated from Mock and MYC-tagged GCase transfected SH-SY5Y cells. The GCase activity was measured using 4-Methylumbelliferyl β -glucophyranoside (n=5, each group).
(S) Confirmation of GCase antibody's quality and integrity. Data are presented as the mean ± SEM (**P* < 0.05, ***P* < 0.01, ****P* < 0.001).

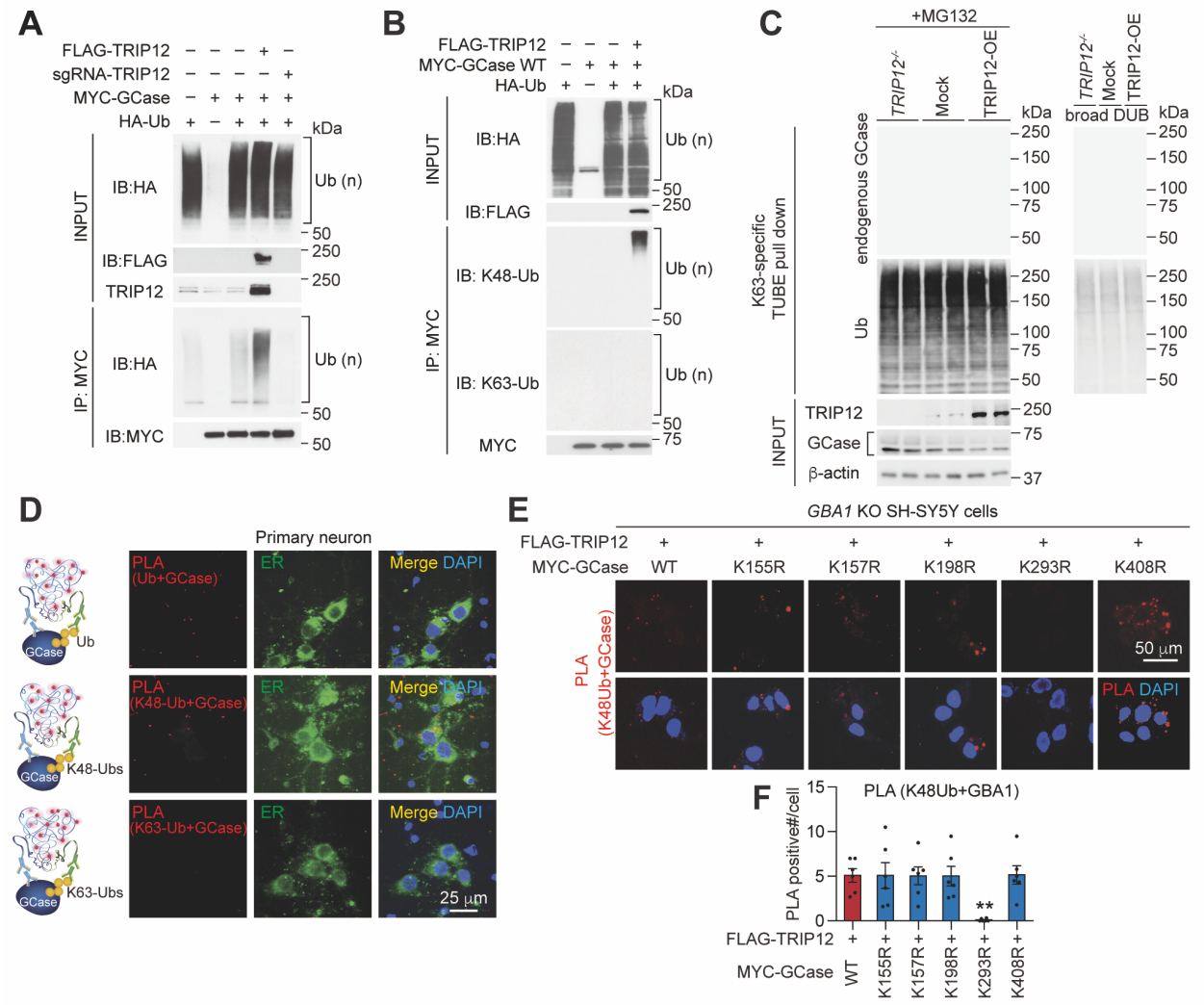

Figure S2. TRIP12 ubiquitinates K293 residue of GCase through K48-specific ubiquitin linkage (Related to Figure 1).

(A) Endogenous TRIP12-induced ubiquitination of MYC-GCase (lane 3 of IP: MYC) was enhanced by FLAG-TRIP12 overexpression but was eliminated in *TRIP12* knockout SH-SY5Y cells (lane 5 of IP: MYC).

(B) In vivo ubiquitination assay, K48-specific ubiquitination of MYC-GCase by FLAG-TRIP12 were confirmed by immunoreactivity with a K48-specific anti-ubiquitin antibody. No immunoreactivity was observed with a K63-specific anti-ubiquitin antibody.

(C) TRIP12 ubiquitinates endogenous GCase through K48-specific ubiquitin linkage. Representative western blots show Ub-MYC-GCase was not detected in fractions enriched by K63-specific TUBE pulldown in SH-SY5Y cells with Mock, TRIP12 overexpression (TRIP12-OE), and *TRIP12* knockout (*TRIP12*$^{-/-}$) in presence of MG132 (left panel). K63-specific ubiquitin enrich fractions were incubated with a DUB (right panel). The isolated ubiquitinated proteins and input material were analyzed anti-GCase, TRIP12, ubiquitin, and β-actin antibodies.

(D) A proximity ligation assays showed that endogenous GCase specifically bound to endogenous K48-specific ubiquitin without any interaction with K63-specific ubiquitin in the ER of primary cultured neurons. The ER was stained with the ER tracker Green. (E) The candidate lysine (K) residues were changed to arginine (R) by site-directed mutagenesis and K48-specific ubiquitination of MYC-GCase WT, MYC-GCase K155R, MYC-GCase K157R, MYC-GCase K198R, MYC-GCase K293R, and MYC-GCase K408R expressed in *GBA1* knockout SH-SY5Y cells were determined by *in situ* PLA assay.
(F) The fluorescence signals were quantified as bar graph. Data are represented as mean ± SEM (NS; not significant, $^{**}P < 0.01$).

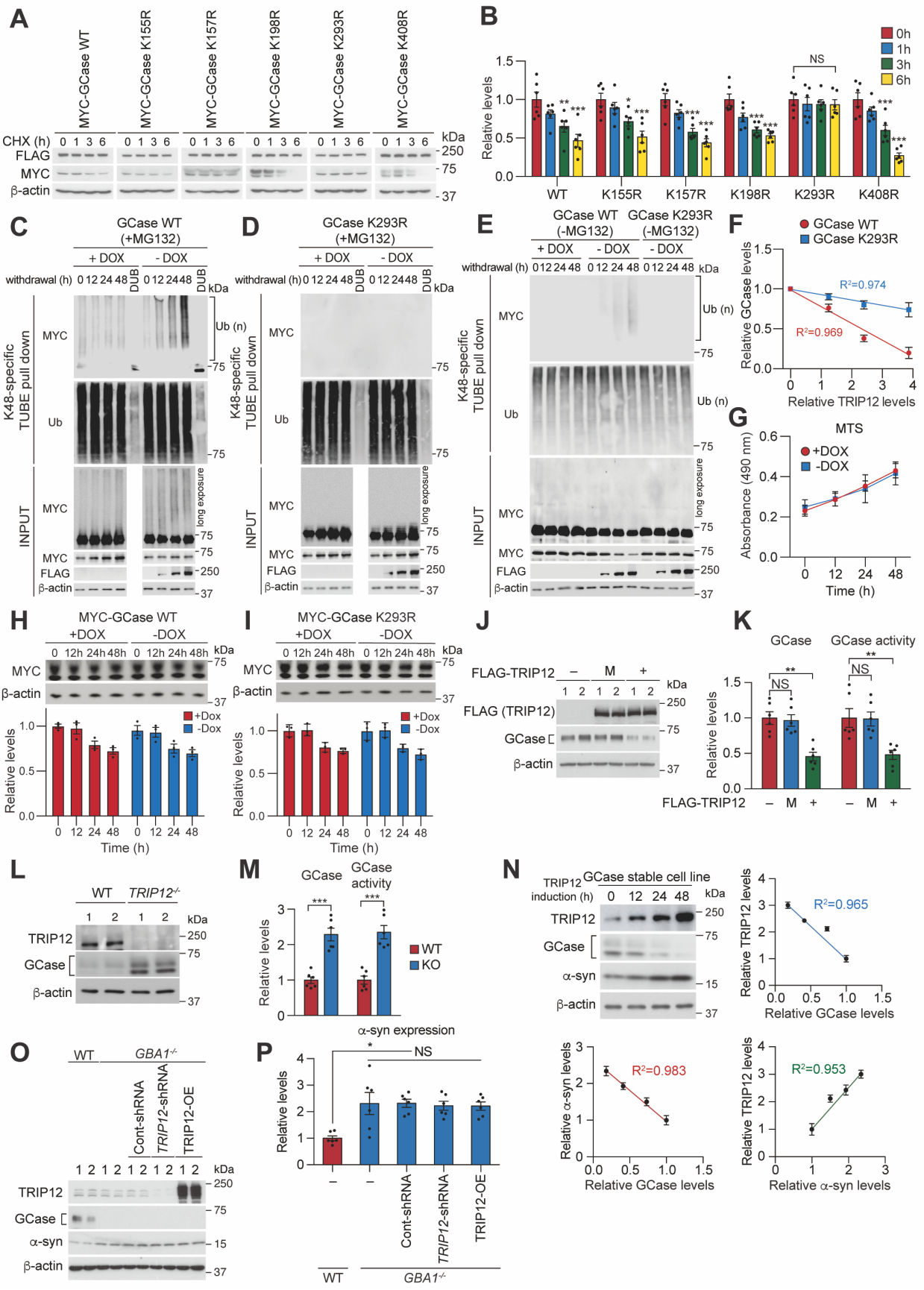
A
MYC-GCase WT
MYC-GCase K155R
MYC-GCase K157R
MYC-GCase K198R
MYC-GCase K293R
MYC-GCase K408R
CHX (h) 0 1 3 6
FLAG
MYC
β-actin
kDa
250
75
37
B
Relative levels
0h
1h
3h
6h
NS
WT
K155R
K157R
K198R
K293R
K408R
C
GCase WT (+MG132)
+ DOX
- DOX
withdrawal (h) 0 12 24 48 DUB
K48-specific TUBE pull down
MYC
Ub
Ub (n)
INPUT
long exposure
D
GCase K293R (+MG132)
E
GCase WT (-MG132)
GCase K293R (-MG132)
F
GCase WT
GCase K293R
Relative GCase levels
R²=0.974
R²=0.969
Relative TRIP12 levels
G
MTS
+DOX
-DOX
Absorbance (490 nm)
Time (h)
H
MYC-GCase WT
+DOX
-DOX
0 12h 24h 48h
MYC
β-actin
+Dox
-Dox
Relative levels
Time (h)
I
MYC-GCase K293R
J
FLAG-TRIP12
–
M
+
FLAG (TRIP12)
GCase
β-actin
K
GCase
GCase activity
NS
Relative levels
L
WT
TRIP12-/-
TRIP12
GCase
β-actin
M
GCase
GCase activity
WT
KO
N
GCase stable cell line
TRIP12 induction (h) 0 12 24 48
TRIP12
GCase
α-syn
β-actin
R²=0.965
Relative TRIP12 levels
Relative GCase levels
R²=0.983
Relative α-syn levels
R²=0.953
O
WT
GBA1-/-
Cont-shRNA
TRIP12-shRNA
TRIP12-OE
P
α-syn expression
Relative levels

Figure S3. TRIP12 site specific ubiquitination of GCase causes its ubiquitin-mediated proteasome degradation, leading to alterations in α-synuclein levels (Related to Figure 1).
(A) MYC-GCase WT, MYC-GCase K155R, MYC-GCase K157R, MYC-GCase K198R, MYC-GCase K293R, and MYC-GCase K408R expression levels were assessed with TRIP12 overexpression in cycloheximide-treated SH-SY5Y cells.
(B) Quantification of MYC-GCase levels (n=6, each group). (C and D) Tet off-inducible FLAG-TRIP12 system in SH-SY5Y cells transfected with
(C) MYC-GCase WT or (D) MYC-GCase K293R in presence of MG132. After the withdrawal of doxycycline, Ub-MYC-GCase was enriched by K48-specific TUBE pulldown. Levels of Ub-MYC-GCase were assessed by western blot at indicated time points (0, 12, 24 h, and 48h). K48-specific ubiquitin enriched fractions at 48h incubated with a DUB. The isolated ubiquitinated proteins and input material were analyzed using anti-MYC, FLAG, ubiquitin, and β-actin antibodies.
(E) Tet off-inducible FLAG-TRIP12 SH-SY5Y cells transfected with MYC-GCase WT or MYC-GCase K293R in absence of MG132. Ub-MYC-GCase in K48-specific ubiquitin enriched fractions and MYC-GCase levels in input materials was evaluated.
(F) Inverse correlation between GCase WT and TRIP12 levels or between GCase K293R and TRIP12 levels.
(G) Cell proliferation in presence or absence of Dox in the Tet off-inducible FLAG-TRIP12 SH-SY5Y cells. The cell proliferation rate was measured at the indicated time points (0, 12 h, 24 h, and 48 h) through MTS assay. Doxycycline (DOX) did not affect cell proliferation in the Tet off-inducible FLAG-TRIP12 SH-SY5Y.
(H and I) Signal decay of transiently expressed GCase according to the presence or absence of DOX in WT SH-SY5Y cells. Western blots and bar graphs showing the signal decay of (H) MYC-GCase WT or (I) MYC-GCase K293R expressed in WT SH-SY5Y over time (0, 12 h, 24 h, and 48 h). GCase constructs showed decreased protein expression by approximately 25%, 48h after transfection regardless of the DOX treatment.
(J and K) GCase expression and GCase activity levels were monitored in FLAG-TRIP12 WT, TRIP12 catalytic site mutant (M) overexpression.
(L and M) GCase expression and GCase activity levels were measured in TRIP12 knockout SH-SY5Y cells (n=6, each group).
(N) TRIP12 was transfected into SH-SY5Y cells stably expressing GCase. The correlation of TRIP12, GCase, and α-synuclein expression levels was determined (n=4, each group). (O) The α-syn expression levels of WT SH-SY5Y cells were compared to those of *GBA1* knockout SH-SY5Y cells with *TRIP12* knockdown (TRIP12-shRNA) or overexpression (TRIP12-OE).
(P) The α-syn expression levels were measured and presented as a bar graph. Data are presented as mean ± SEM (NS; not significant, $*P < 0.05$, $**P < 0.01$, $***P < 0.001$).

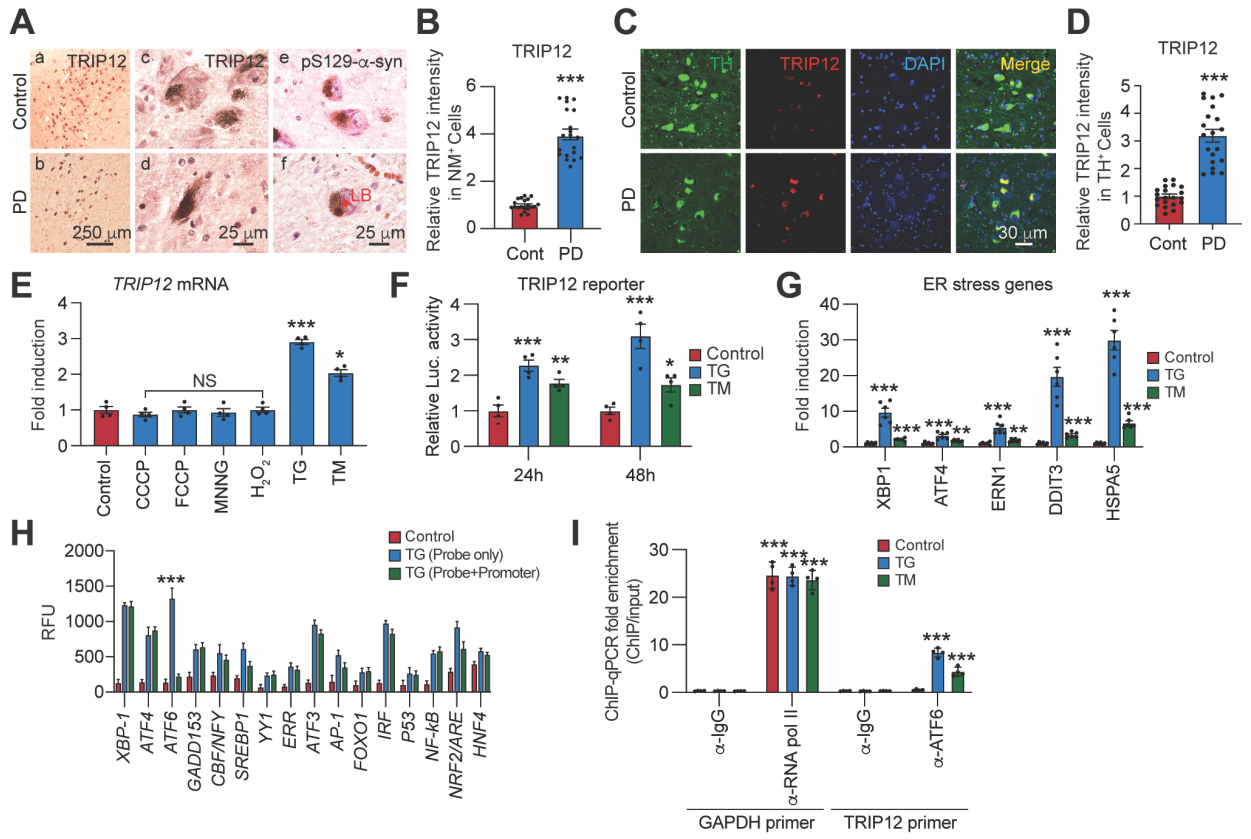

Figure S4. TRIP12 increases in the dopaminergic neurons in the SN of human PD postmortem brain and ER stress induces TRIP12 expression via transcription factor ATF6 (Related to Figure 2).

(A) Representative images showing the TRIP12 accumulation in the neuromelanin-positive (NM^+) dopaminergic neurons of the SNpc of human PD postmortem brain.

(B) Quantitation of the TRIP12 levels from the pigmented dopaminergic neurons of the SNpc (n=20, each group).

(C) Representative images showing the TRIP12 accumulation in the TH-positive (TH^+) dopaminergic neurons of the SNpc of human PD postmortem brain.

(D) Quantitation of the TRIP12 levels from the TH^+ dopaminergic neurons of the SNpc (n=20, each group).

(E) *TRIP12* mRNA expression is upregulated in SH-SY5Y cells after 2 hours by ER stress-inducing reagent, thapsigargin (TG; 1 mM) or tunicamycin (TM; 1 mg/ml), but not by Carbonylcyanide-3-chlorophnylhydrazone (CCCP; 10 μM) and carbonylcyanide-4 trifluoromethoxyphenylhydrazone (FCCP; 1 μM) provoked mitochondrial dysfunction; methylinitronitrosoguanidine (MNNG; 100 μM) induced DNA damage or hydrogen peroxide (100 μM) generated oxidative stress.

(F) The luciferase reporter assay shows that ER stress-inducing reagents increase *TRIP12* at the transcriptional level.

(G) The expression of ER stress-related genes (*XBP1*, *ATF4*, *ERN1*, *DDIT3*, and *HSPA5*) are increased in TG or TM treated SH-SY5Y cells.
(H) Transcription factors for TRIP12 expression were screened using an ER-related promoter binding transcription factor profiling assay.
(I) The involvement of transcription factor ATF6 in *TRIP12* gene regulation was confirmed with a ChIP assay. Data are represented as the mean ± SEM (NS; not significant, $^{*}P < 0.05$, $^{**}P < 0.01$, $^{***}P < 0.001$).

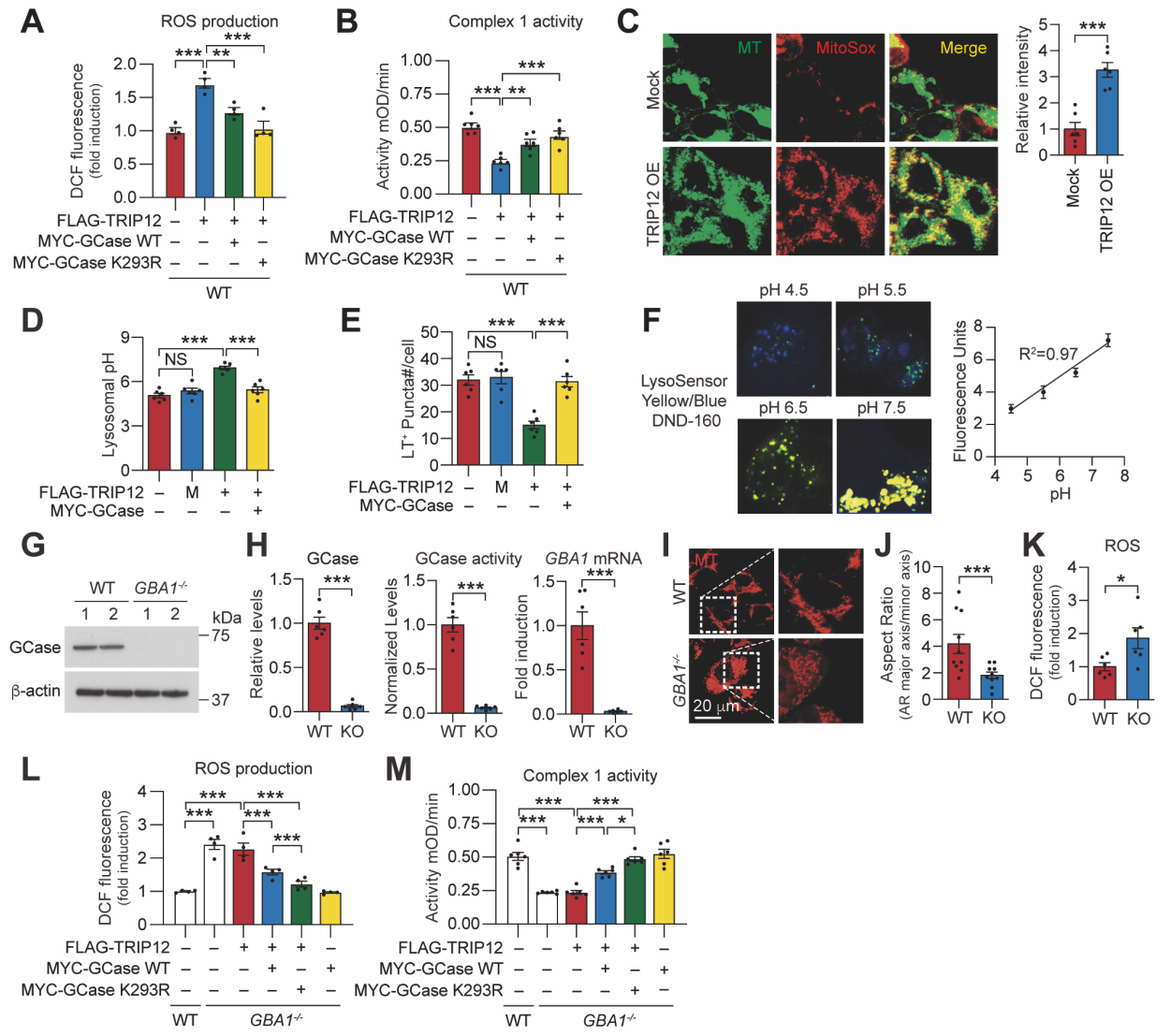

Figure S5. TRIP12 accumulation causes mitochondria dysfunction via GCase-dependent manner (Related to Figure 3).

(A and B) WT SH-SY5Y cells were transfected with only FLAG-TRIP12, both FLAG-TRIP12 and MYC-GCase WT, or both FLAG-TRIP12 and MYC-GCase K293R.

(A) Bar graph of ROS production (n=4, each group)

(B) Bar graph of Mitochondrial complex I activity (n=4, each group).

(C) Mitochondria-derived ROS was assessed by MitoSox staining and represented in bar graph.

(D) The lysosomal pH was measured using LysoSensor and represented in bar graph. (E) The number of Lysotracker-positive puncta per cell was measured and represented in bar graph.

(F) A standard graph to evaluate lysosomal pH.

(G) GCase expression levels were assessed in *GBA1* knockout SH-SY5Y cells by western blot analysis.

(H) GCase levels, GCase activity, and *GBA1* mRNA expression levels were represented as bar graphs (n=6, each group).

(I) Mitotracker (MT; Red) were used to stain mitochondria, respectively, in WT or *GBA1* knockout SH-SY5Y cells. Mitochondrial fragmentation was detected in *GBA1* knockout SH-SY5Y cells.
(J) Mitochondrial aspect ratio was calculated in WT or *GBA1* knockout SH-SY5Y cells (n=10, each group).
(K) ROS production was measured and represented as a bar graph (n=6, each group).
(L and M) *GBA1* knockout SH-SY5Y cells were transfected with only FLAG-TRIP12, MYC-GCase, both FLAG-TRIP12 and MYC-GCase WT, or both FLAG-TRIP12 and MYC-GCase K293R.
(L) Bar graph of ROS production (n=4, each group).
(M) Bar graph of Mitochondrial complex I activity (n=4, each group). Data are represented as mean ± SEM (NS; not significant, *P < 0.05, **P < 0.01, ***P < 0.001).

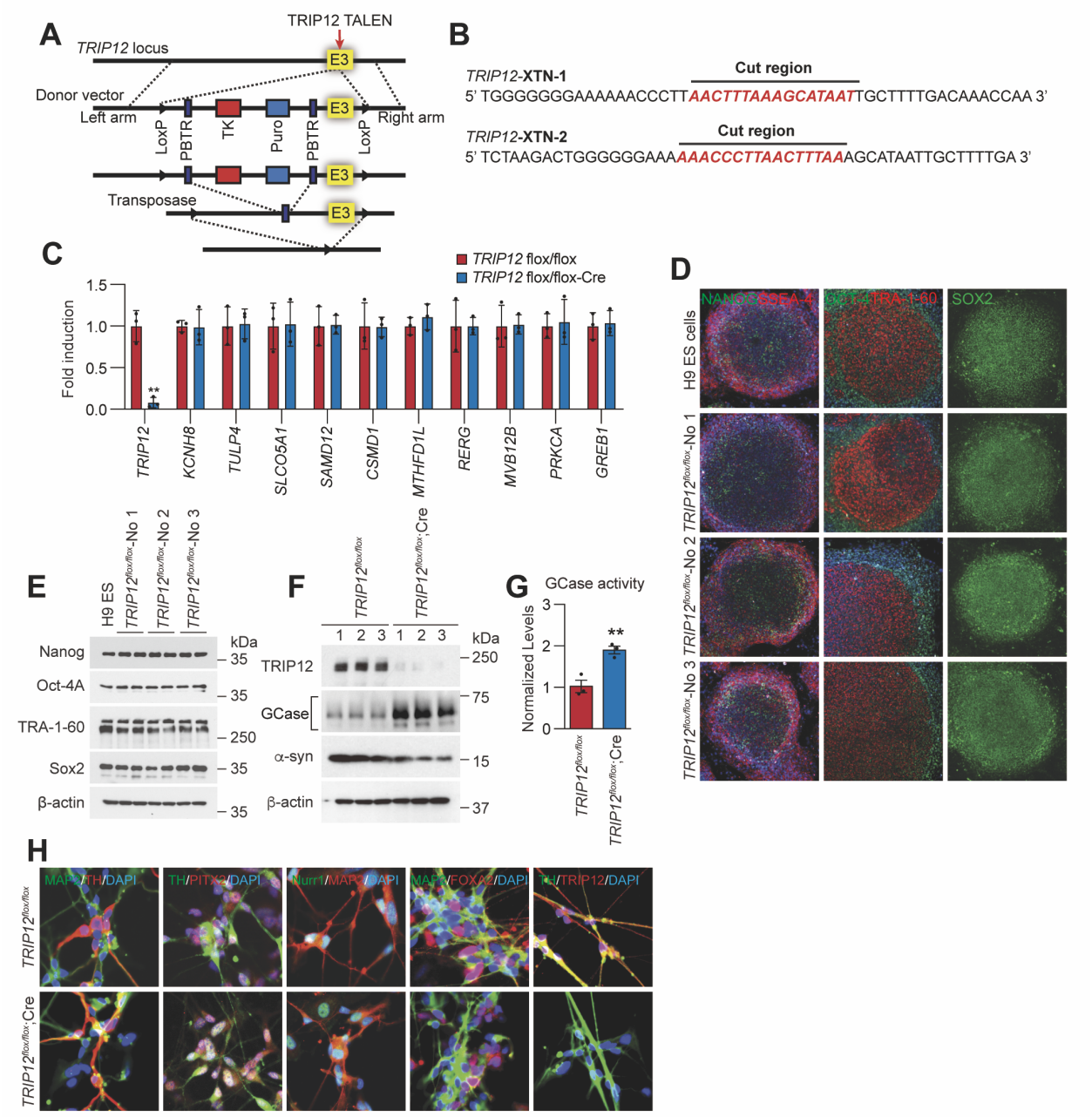

Figure S6. Generation and characterization of conditional *TRIP12* knockout ES-derived human DA neurons (Related to Figure 5).

(A and B) Schematic diagram of the transcription activator-like effector nuclease (TALEN)-based *TRIP12* knockout construction and specific target sequences.

(C) The evaluation of off-target effects in *TRIP12* ES knock-out line.

(D) Conditional *TRIP12* knockout (*TRIP12*$^{flox/flox}$;Cre) ES cell lines were characterized by staining for the endogenous pluripotent markers NANOG, SSEA-4, OCT-4, TRA-1-60, and SOX2.

(E) Western blot with anti-NANOG, anti-OCT-4A, anti-TRA-1-60, and anti-Sox2 in *TRIP12* conditional knockout (TRIP12$^{flox/flox}$;Cre) ES cell lines.

(F) TRIP12, GCase, and α-syn expression levels the Human ES cells after 60 days of maturation to DA neurons.
(G) GCase activity.
(H) After maturation, DA neurons were confirmed by the neuronal markers TH, PITX2, Nurr1, and FOXA2. The TRIP12 expression was confirmed in Control (*TRIP12*$^{flox/flox}$) and was absent in *TRIP12* knockout (*TRIP12*$^{flox/flox}$;Cre) human DA neurons. Data are presented as the mean ± SEM (NS; not significant, $^{*}P < 0.05$, $^{**}P < 0.01$, $^{***}P < 0.001$).

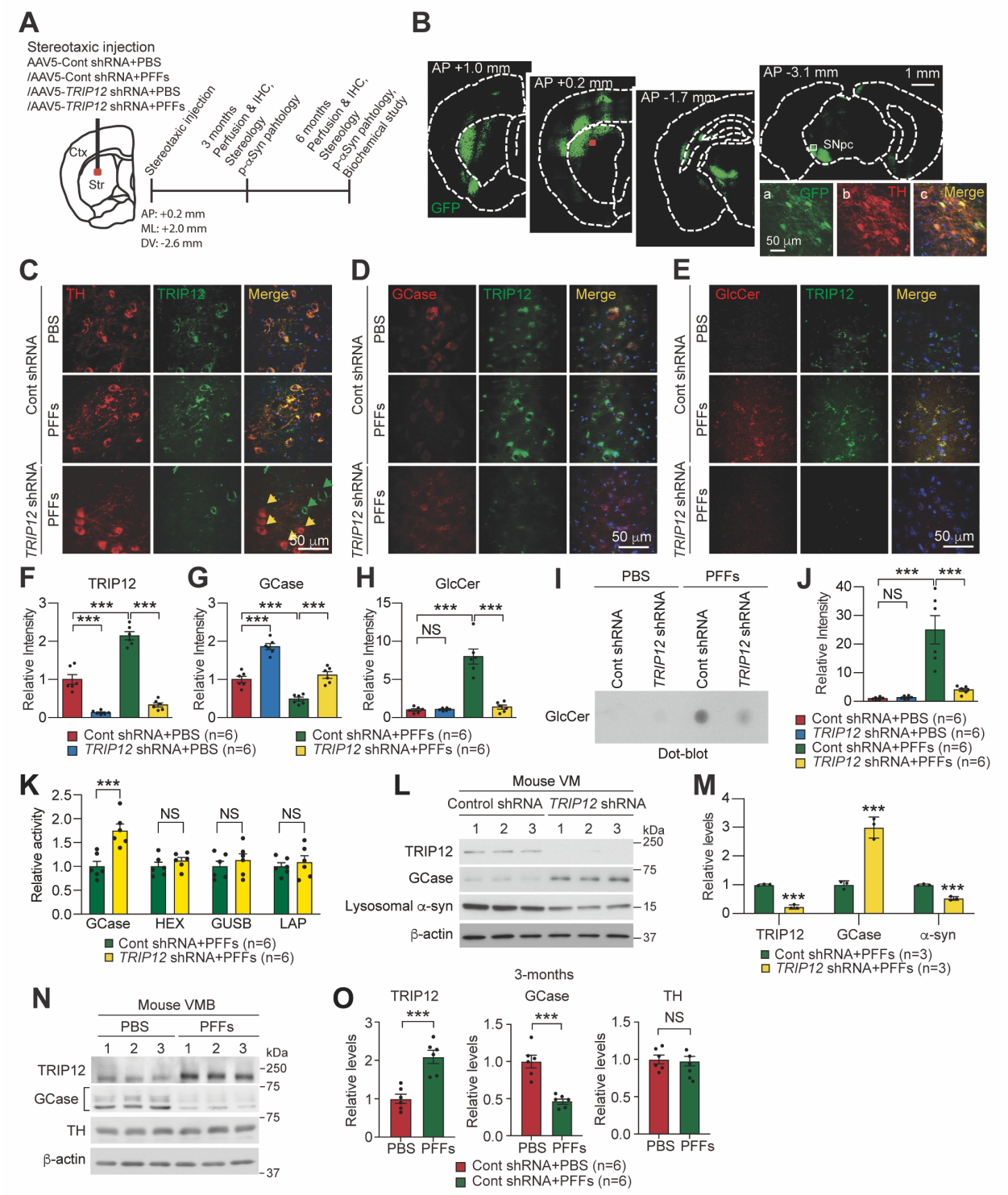

Figure S7. *TRIP12* Knockdown protects against α-synuclein PFFs-induced neurodegeneration *in vivo* (Related to Figure 7).

(A) A schematic illustration of stereotaxic intrastriatal injection.

(B) GFP expression in the SNpc at 1-month post-injection of AAV5-Cont shRNA.

(C) Representative confocal images of TRIP12 (green) in TH-positive cells (red) of the SNpc of PBS or α-syn PFFs injected mice transduced with AAV5-Cont shRNA (Cont shRNA) or AAV5-TRIP12 shRNA (TRIP12 shRNA).
(D) GCase (red) and TRIP12 (green) were stained in the SNpc of mice.
(E) GlcCer (red) and TRIP12 (green) were stained in the SNpc of mice.
(F-G) Bar graph of fluorescence intensity of TRIP12, GCase, and GlcCer.
(I and J) GlcCer levels were determined via dot-blot with an anti-GlcCer antibody.
(K) The activities of lysosomal hydrolases such as GCase, hexosaminidase A/B/C (HEX), β-glucuronidase (GUSB), and lysosomal acid phosphatase (LAP) were measured in the VMB of α-syn PFFs-injected mice with or without *TRIP12* knockdown and represented in bar graph.
(L and M) The expression of TRIP12, GCase, and lysosomal α-syn expression levels measured in the VMB of α-syn PFFs-injected mice with or without *TRIP12* knockdown by western blot and represented in bar graph.
(N and O) TRIP12, GCase, and TH levels in the VMB of mice at 3-months after α-syn PFFs injection without *TRIP12* knockdown.
(N) Representative western blots showing TRIP12, GCase, TH, and α-syn levels from the ventral midbrain of α-syn PFFs-injected mice.
(O) Protein levels were quantified as bar graphs. (n=6, each group). Data are represented as mean ± SEM (NS; not significant, ***$P < 0.001$).

SUPPLEMENTAL TABLE

Table S1. GCase binding proteins by Tandem affinity purification analysis (Related to Figure 1).

No	SwissProt Acc Nr	Protein Name	M.W. (Da)	Matches Peptide Signals	Unique Peptide (MS/MS)	Unique Peptide ion score	Coverage (%)
1	GLCM_HUMAN	Glucosylceramidase	60,134	75	14	1514	28.40
2	TRIPC_HUMAN	Probable E3 ubiquitin-protein ligase TRIP12 (GUMP)	222,234	39	3	39	1.00
3	TBB2C_HUMAN	Tubulin beta-2C chain	50,255	17	9	248	24.00
4	TBA1B_HUMAN	Tubulin alpha-1B chain	50,804	16	9	297	26.60
5	TBA3E_HUMAN	Tubulin alpha-3E chain	50,568	14	7	232	21.80
6	TBB3_HUMAN	Tubulin beta-3 chain	50,856	13	7	229	19.10
7	CALX_HUMAN	Calnexin	67,982	12	6	191	13.70
8	TBB2A_HUMAN	Tubulin beta-2A chain	50,274	11	6	179	16.60
9	TBB8_HUMAN	Tubulin beta-8 chain	50,257	10	5	164	13.30
10	HSP72_HUMAN	Heat shock-related 70 kDa protein 2	70,263	7	3	250	6.70
11	POTEE_HUMAN	POTE ankyrin domain family member E	122,882	6	3	100	3.50
12	EF1A2_HUMAN	Elongation factor 1-alpha 2	50,780	6	3	69	10.80
13	IAH1_HUMAN	Isoamyl acetate-hydrolyzing esterase 1 homolog	28,037	6	1	38	5.60
14	KI67_HUMAN	Antigen KI-67	360,698	6	6	25	2.90
15	SVIL_HUMAN	Supervillin	249,417	6	6	17	3.50
16	GFAP_HUMAN	Glial fibrillary acidic protein	49,907	5	3	113	7.20
17	RAE1_HUMAN	Rab proteins geranylgeranyltransferase component A 1	74,740	5	2	34	3.40
18	FHAD1_HUMAN	Forkhead-associated domain-containing protein 1	162,659	4	2	47	1.80
19	WDR52_HUMAN	WD repeat-containing protein 52	112,571	4	1	26	1.90
20	OPA1_HUMAN	Dynamin-like 120 kDa protein, mitochondrial	112,131	4	3	23	3.20
21	GPBP1_HUMAN	Vasculin	53,478	4	1	17	1.90
22	HSP76_HUMAN	Heat shock 70 kDa protein 6	71,440	3	3	126	6.70
23	UDB15_HUMAN	UDP-glucuronosyltransferase 2B15	61,510	3	1	51	2.50
24	EEA1_HUMAN	Early endosome antigen 1	163,337	3	2	48	1.90
25	CQ104_HUMAN	Uncharacterized protein C17orf104	108,689	3	2	44	2.60
26	TRAP1_HUMAN	Heat shock protein 75 kDa, mitochondrial	80,345	3	3	40	8.10
27	H2A1A_HUMAN	Histone H2A type 1-A	14,225	3	1	37	6.90
28	3BHS1_HUMAN	3 beta-hydroxysteroid dehydrogenase/Delta 5-->4-isomerase ty	42,510	3	1	17	2.40
29	FMR1N_HUMAN	Fragile X mental retardation 1 neighbor protein	29,792	3	1	17	3.50
30	NTRK1_HUMAN	High affinity nerve growth factor receptor	88,639	3	3	17	2.60
31	IRX5_HUMAN	Iroquois-class homeodomain protein IRX-5	50,672	3	1	17	1.70
32	SPIN1_HUMAN	Spindlin-1	29,696	3	3	17	19.80
33	CE290_HUMAN	Centrosomal protein of 290 kDa	290,892	3	3	14	1.70
34	MYLK2_HUMAN	Myosin light chain kinase 2, skeletal/cardiac muscle	65,214	2	2	67	1.80
35	SETB1_HUMAN	Histone-lysine N-methyltransferase SETDB1	145,119	2	1	56	0.60
36	HNRPD_HUMAN	Heterogeneous nuclear ribonucleoprotein D0	38,581	2	2	55	9.30
37	HS90A_HUMAN	Heat shock protein HSP 90-alpha	85,006	2	2	40	3.60
38	RHDF1_HUMAN	Inactive rhomboid protein 1	98,935	2	1	38	1.20
39	MYH13_HUMAN	Myosin-13	224,605	2	2	35	1.90
40	DJB13_HUMAN	DnaJ homolog subfamily B member 13	36,267	2	1	30	2.80
41	ZN273_HUMAN	Zinc finger protein 273	66,868	2	2	25	2.80
42	TBA4B_HUMAN	Putative tubulin-like protein alpha-4B	27,819	2	1	24	5.00
43	VP13D_HUMAN	Vacuolar protein sorting-associated protein 13D	495,298	2	2	24	0.70
44	DGKZ_HUMAN	Diacylglycerol kinase zeta	125,704	2	2	23	2.10
45	S12A7_HUMAN	Solute carrier family 12 member 7	120,283	2	2	19	2.20
46	ZN175_HUMAN	Zinc finger protein 175	84,009	2	2	19	3.70
47	DEN4C_HUMAN	DENN domain-containing protein 4C	188,563	2	2	18	2.00
48	DAXX_HUMAN	Death domain-associated protein 6	82,064	2	1	17	1.20
49	CATC_HUMAN	Dipeptidyl peptidase 1	52,619	2	2	17	3.20
50	MYH8_HUMAN	Myosin-8	223,594	2	2	17	0.90
51	POTEM_HUMAN	Putative POTE ankyrin domain family member M	58,000	2	2	17	7.10
52	SNX25_HUMAN	Sorting nexin-25	98,625	2	2	17	1.80
53	VP13C_HUMAN	Vacuolar protein sorting-associated protein 13C	424,462	2	2	17	0.20
54	K1462_HUMAN	Uncharacterized protein KIAA1462	149,343	2	2	16	1.50

Table S2. Identification of GCase's ubiquitination sites and ubiquitin linkages (Related to Figure 1 and Figure S2).

Protein identity	Ubiquitination sites of GBA1 (The number of Uniquitinated lysine residues)					Protein coverage by amino acid count
GBA1	MEFSSPSREE	CPKPLSRVSI	MAGSLTGLLL	LQAVSWASGA	RPCIPKSFGY	375/536 = 69.96 %
	SSVVCVCNAT	YCDSFDPPTF	PALGTFSRYE	STRSGRRMEL	SMGPIQANHT	
	GTGLLLTLQP	EQKFQKVKGF	GGAMTDAAAL	NILALSPPAQ	NLLLKSYFSE	
	EGIGYNIIRV	PMASCDFSIR	TYTYADTPDD	FQLHNFSLPE	EDTKLKIPLI	
	HRALQLAQRP	VSLLASPWTS	PTWLKTNGAV	NGKGSLKGQP	GDIYHQTWAR	
	YFVKFLDAYA	EHKLQFWAVT	AENEPSAGLL	SGYPFQCLGF	TPEHQRDFIA	
	RDLGPTLANS	THHNVRLLML	DDQRLLLPHW	AKVVLTDPEA	AKYVHGIAVH	
	WYLDFLAPAK	ATLGETHRLF	PNTMLFASEA	CVGSKFWEQS	VRLGSWDRGM	
	QYSHSIITNL	LYHVVGWTDW	NLALNPEGGP	NWVRNFVDSP	IIVDITKDTF	
	YKQPMFYHLG	HFSKFIPEGS	QRVGLVASQK	NDLDAVALMH	PDGSAVVVVL	
	NRSSKDVPLT	IKDPAVGFLE	TISPGYSIHT	YLWRRQ		
	(Total 5 ubiquitination sites)					

Signal peptide

Uniquitination site (K155, K157, K198, K293, K408)

Protein identity	Ubiquitination sites of Ub (The number of Uniquitinated lysine residues)					Protein coverage by amino acid count
Ubiquitin	MQIFVKTLTG	KTITLEVEPS	DTIENVKAKI	QDKEGIPPDQ	QRLIFAGKQL	70/76 = 92.11 %
	EDGRTLSDYN	IQKESTLHLV	LRLRGG			

Ubiquitination site (K11, K48)

* Red type K letters indicate ubiquitinated Lysine residues on GBA1 or ubiquitin.

Table S3. Human post-mortem tissues used in Figure 2 and Figure S4

Human Substantia nigra postmortem

Case#	Age	Sex	Race	PMD	Diagnosis	Genotype	Immunoblotting	Immunohistochemistry (IHC)
713	73	F	W	9	Control	WT	O	
935	79	M	W	16	Control	WT	O	
2052	79	M	W	16	Control	WT	O	O
2193	89	M	W	8.5	Control	WT	O	O
289	68	F	W	35	Control	WT	O	
507	87	F	W	23	Control	WT	O	O
2071	76	M	W	17	PD with Dementia	WT	O	
2091	83	F	W	4	PD with Dementia	WT	O	O
2138	83	M	W	5	PD with Dementia	WT	O	O
2140	84	F	W	9	PD with Dementia	WT	O	O
2165	80	F	W	16	PD with Dementia	WT	O	
2544	89	M	W	16	PD with Dementia	WT	O	